Organometallics **2006,** *25,* 4170−4178

Divalent Germanium and Tin Compounds Stabilized by Sterically Bulky P^O, P═O^O, P═S^O, and P═N^O Ligands: Synthesis and First Insights into Catalytic Application to Polyurethane Systems[†]

Alex S. Ionkin,* William J. Marshall, and Brian M. Fish

DuPont Central Research & Development, Experimental Station, Wilmington, Delaware 19880-0328

Received April 21, 2006

A sterically bulky chelating phosphine, $^t\mathrm{Bu_2P{-}CH_2{-}C(CF_3)_2OH}$ (**1**), was shown to stabilize divalent tin and germanium compounds: $\mathrm{M[{-}O{-}C(CF_3)_2CH_2P^tBu_2]_2}$ (**6**, M = Sn; **14**, M = Ge). Oxidizing reagents, e.g., sulfur, pyridine-*N*-oxide, and 1-azidoadamantane, reacted with divalent tin **6** on the phosphorus ligands exclusively, preserving the divalent state of tin in the resultant compounds $\mathrm{Sn[{-}O{-}C(CF_3)_2CH_2P(S)^tBu_2]_2}$ (**7**), $\mathrm{Sn[{-}O{-}C(CF_3)_2CH_2P(O)^tBu_2]_2}$ (**11**) and $\mathrm{Sn[{-}O{-}C(CF_3)_2CH_2P^tBu_2],[{-}O{-}C(CF_3)_2CH_2P(N_3\text{-}Adamantyl)^tBu_2]_2}$ (**12**). The divalent germanium compound **14** was found to be more prone to oxidation to the tetravalent state. For example, the reaction with 1-azidoadamantane gave tetravalent germanium compounds $\mathrm{Ge[{-}O{-}C(CF_3)_2CH_2P({-})^tBu],[\text{-}O{-}C(CF_3)_2CH_2P({=}N\text{-})^tBu_2]}$ (**16**) and $\mathrm{[Adamantyl],[{-}O{-}C(CF_3)_2CH_2P({=}N{-})]Ge{-}O{-}Ge[{-}O{-}C(CF_3)_2CH_2P(^tBu)_2({=}N{-})],[Adamantyl]}$ (**17**). A Ge−O−Ge bridge in **17** is very linear, with an angle Ge−O−Ge of 177.4(2)°. According to X-ray analyses the intramolecular M−P bond lengths are among the longest known for this kind of bonding: 3.228(4) Å for P−Sn in **12** and 2.7585(12) Å for P−Ge in **14**. The divalent tin compounds **6** and **7** were found to be efficient catalysts for the formation of polyurethanes. The divalent germanium compound **14** was active in polyurethane formation, but it was an order of magnitude less active than corresponding tin analogue **6**.

Introduction

The first stable germanium and tin organometallic analogues of carbenes $\mathrm{[(Me_3Si)_2CH]_2M}$ (M = Ge, Sn) were synthesized 30 years ago by Lappert and co-workers.[1] Since then, considerable progress has been made in the stabilization of such compounds via kinetic and thermodynamic methodologies.[2] The syntheses of some milestone classes of heavier carbene analogues should also be mentioned: the sterically stabilized aryloxy derivatives,[3] 2,4,6-tris(trifluoromethyl)phenyl derivatives,[3c] 2,4,6-tri-*tert*-butylphenyl derivatives[3d] (types **A**, **B**, and **C** in Scheme 1), bis(tris(trimethylsilyl)silyl)stannylene[4] (type **D**), divalent germanium and tin compounds containing a bulky diketiminato ligand[5] (type **E**), and divalent tin and germanium compounds stabilized by intramolecular coordination with nitrogen[6] (type **F**).

Scheme 1

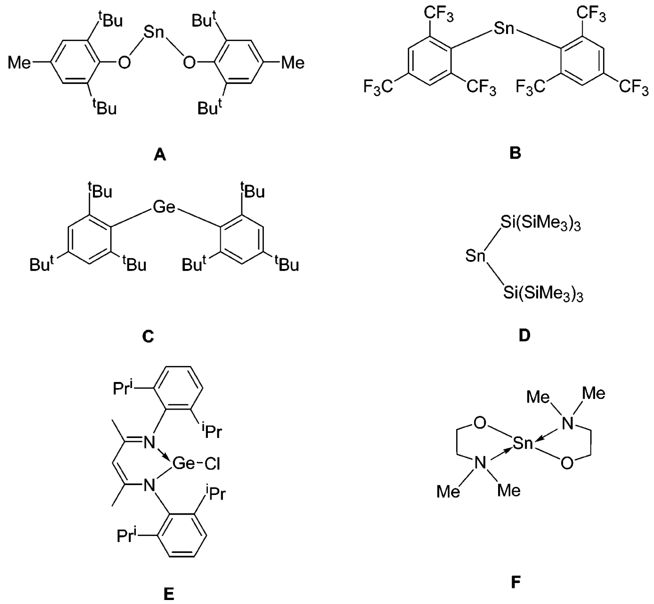

A new chelating phosphine, $^t\mathrm{Bu_2P{-}CH_2{-}C(CF_3)_2OH}$ (**1**), with a sterically bulky "soft" di-*tert*-butyl phosphine center and bulky "hard" fluorinated alkoxy center has been shown previously to stabilize unusual coordination numbers of iridium, e.g., the rare mononuclear divalent iridium complex **2**, a coordinately

---

[†] This is DuPont contribution no. 8669.

* To whom correspondence should be addressed. E-mail: alex.s.ionkin@usa.dupont.com.

(1) (a) Goldberg, D. E.; Harris, D. H.; Lappert, M. F.; Thomas, K. M. *Chem. Commun.* **1976**, *7*, 261. (b) Davidson, P. J.; Harris, D. H.; Lappert, M. F. *J. Chem. Soc., Dalton Trans.* **1976**, *21*, 2268. (c) Hitchcock, P. B.; Lappert, M. F.; Miles, S. J.; Thorne, A. J. *Chem. Commun*. **1984**, *7*, 480.

(2) (a) Tokitoh, N.; Okazaki, R. *Coord. Chem. Rev.* **2000**, *210*, 251. (b) Tzschach, A.; Jurkschat, K.; Scheer, M. *Nova Acta Leopold.* **1985**, *59*, 305. (c) Takeda, N.; Tokitoh, N.; Okazaki, R. *Sci. Synth.* **2003**, *5*, 311. (d) Podlech, J. *Sci. Synth.* **2003**, *5*, 273.

(3) (a) Cetinkaya, B.; Gumrukcu, I.; Lappert, M. F.; Atwood, J. L.; Rogers, R. D.; Zaworotko, M. J. *J. Am. Chem. Soc.* **1980**, *102*, 2088. (b) Braunschweig, H.; Hitchcock, P. B.; Lappert, M. F.; Pierssens, L. J. M. *Angew. Chem., Int. Ed. Engl.* **1994**, *33*, 1156. (c) Takeda, N.; Tokitoh, N.; Okazaki, R. *Sci. Synth.* **2003**, *5*, 311. (d) Takeda, N.; Tokitoh, N.; Okazaki, R. *Sci. Synth.* **2003**, *5*, 51.

(4) (a) Klinkhammer, K. W.; Schwarz, W. *Angew. Chem., Int. Ed. Engl.* **1995**, *43*, 1334. (b) Klinkhammer, K. *Polyhedron* **2002**, *21*, 587. (c) Klinkhammer, K. W.; Fassler, T. F.; Grutzmacher, H. *Angew. Chem., Int. Ed.* **1998**, *37*, 124.

(5) (a) Ding, Y.; Roesky, H. W.; Noltemeyer, M.; Schmidt, H.-G.; Power, P. P. *Organometallics* **2001**, *20*, 1190. (b) Pineda, L. W.; Jancik, V.; Roesky, H. W.; Neculai, D.; Neculai, A. M. *Angew. Chem., Int. Ed.* **2004**, *43*, 1419. (c) Ding, Y.; Ma, Q.; Roesky, H. W.; Herbst-Irmer, R.; Uson, I.; Noltemeyer, M.; Schmidt, H.-G. *Organometallics* **2002**, *21*, 5216.

10.1021/om060355c CCC: $33.50

Scheme 2

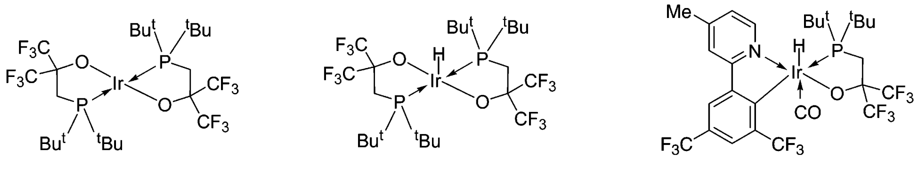

2 3 4

Scheme 3

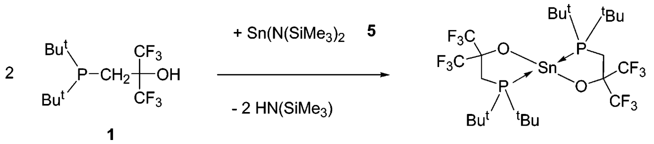

1 6

unsaturated monohydride **3**, and a monocyclometalated complex **4** (Scheme 2).[7]

This report describes the application of the P^O chelating phosphine **1** to the stabilization of divalent tin and germanium compounds as well as the reactivity of isolated products and their application as catalysts for the formation of polyurethanes.

Results and Discussion

1.1. Synthesis, Reactivity, and Structural Studies of Divalent Tin Compounds. The reaction between 2-[(di-*tert*-butylphosphino)methyl]-1,1,1,3,3,3-hexafluoropropan-2-ol (**1**) and bis[bis(trimethylsilyl)amino]tin(II) (**5**) at room temperature afforded the divalent tin compound **6**, containing two chelating five-membered rings (Scheme 3).

The ^{31}P NMR resonance of **6** was not significantly shifted downfield upon coordination to tin ($\delta = 5.8$ ppm for **1** and 18.2 ppm for **6**). This may indicate weak coordination to tin. (The ^{31}P NMR resonance of iridium complex **3**, for example, is at 80.3 ppm, a downfield shift of 74.5 ppm.) The observation of ^{119}Sn satellites on either side of the ^{31}P NMR resonance of **6** ($^{1}J_{\mathrm{P119Sn}} = 865.4$ Hz) confirms the presence of a direct P−Sn bond.[8] The ^{119}Sn NMR chemical shift for **6**, 292 ppm, is characteristic of tetracoordinate tin compounds containing at least one Sn−O bond.[6,9]

The structure of **6** was determined by single-crystal X-ray diffraction (Figure 1).

The geometry about the tin atom in **6** is pyramidal, with the phosphorus and oxygen atoms forming the base and the tin atom situated at the apex. The Sn−P bond lengths in **6** (2.8376 and 2.8460 Å, Table 1) are the second longest of 42 tetracoordinate analogues falling in the range between 2.41[10] and 3.04 Å[11] (Cambridge Structural Database).

The electron-rich molecule **6** has several centers with which to react with electrophiles: the divalent tin and the two phosphorus atoms. It is difficult to predict oxidation pathways for such compounds. For example, in the oxidation reaction of **6** by sulfur, the two phosphorus atoms are oxidized, but not the tin atom (Scheme 4).

Table 1. Selected Bond Lengths (Å) and Angles (deg) for 6 (M = Sn) and 14 (M = Ge)

	Sn (**6**)	Ge (**14**)
M−O1	2.118(3)	1.906(3)
M−O2	2.128(3)	1.910(3)
M−P1	2.8376(12)	2.7331(12)
M−P2	2.8460(11)	2.7585(12)
O1−M−O2	104.67(11)	96.78(14)
O1−M−P2	82.20(8)	87.56(9)
O2−M−P2	71.19(8)	75.26(9)
O1−M−P1	71.17(8)	75.21(10)
O2−M−P1	82.75(8)	87.15(9)
P2−M−P1	136.43(3)	153.80(4)

Scheme 4

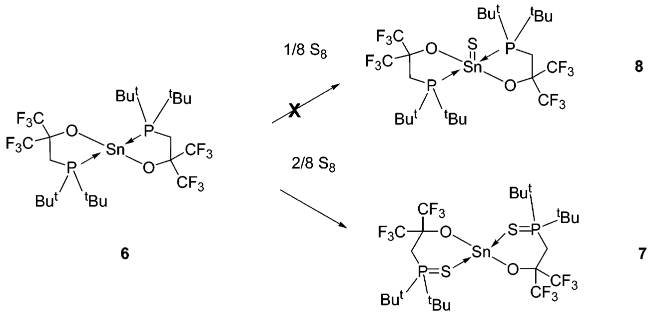

The tin(II) complex **7** was isolated as the sole product with a yield of 97% from this reaction. A product of divalent tin oxidation, e.g., **8**, was not observed.

The ^{31}P NMR spectrum of **7** consists of a singlet at 67.11 ppm with satellite couplings ($^{2}J_{\mathrm{P119Sn}} = 114.4$ Hz). The

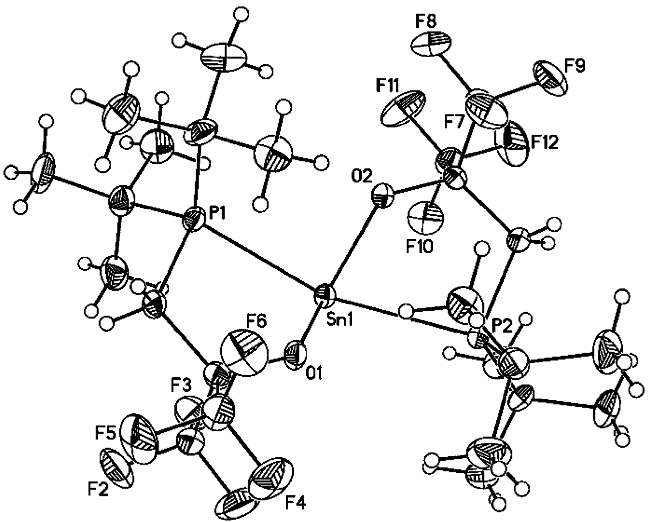

Figure 1. ORTEP drawing of tin(II), *trans*-bis[3-(di-*tert*-butylphosphino)-1,1,1-trifluoro-2-(trifluoromethyl)-2-propanolato-*O,P*]-, **6**.

---

(6) (a) Jolly, B. S.; Lappert, M. F.; Engelhardt, L. M.; White, A. H.; Raston, C. L. *J. Chem. Soc., Dalton Trans.* **1993**, *17*, 2653. (b) Zemlyansky, N. N.; Borisova, I. V.; Kuznetsova, M. G.; Khrustalev, V. N.; Ustynyuk, Y. A.; Nechaev, M. S.; Lunin, V. V.; Barrau, J.; Rima, G. *Organometallics* **2003**, *22*, 1675. (c) Khrustalev, V. N.; Antipin, M. Yu.; Zemlyansky, N. N.; Borisova, I. V.; Ustynyuk, Y. A.; Lunin, V. V.; Barrau, J.; Rima, G. *J. Organomet. Chem.* **2004**, *689*, 478.

(7) Ionkin, A. S.; Marshall, W. J. *Organometallics* **2004**, *23*, 6031.

(8) (a) Heckmann, G.; Binder, H.; Bongert, D. *Magn. Reson. Chem.* **1998**, *36*, 250. (b) Yoder, C. H.; Margolis, L. A.; Horne, J. M. *J. Organomet. Chem.* **2001**, *633*, 33.

(9) Braunschweig, H.; Chorley, W. R.; Hitchcock, P. B.; Lappert, M. F. *Chem. Commun.* **1992**, 1311.

(10) Schaller, A.; Hausen, H.-D.; Schwarz, W.; Heckman, G.; Weidlein, J. *Z. Anorg. Allg. Chem.* **2000**, *626*, 1047.

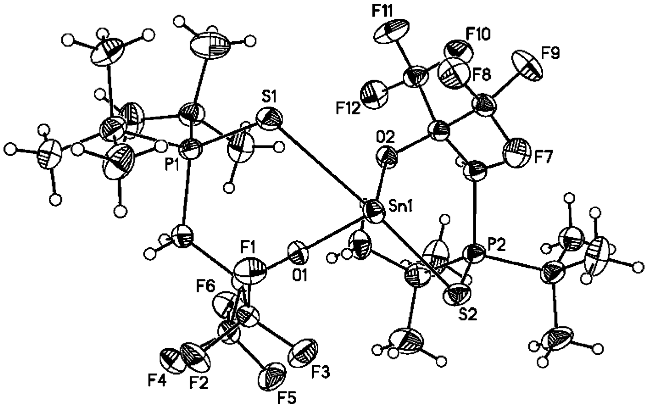

Figure 2. ORTEP drawing of tin(II), *trans*-bis[3-(di-*tert*-butylphosphinothioyl)-1,1,1-trifluoro-2-(trifluoromethyl)-2-propanolato-*κO,κS*]-, **7**. Selected bond lengths (Å): Sn−O1 = 2.0810(16), Sn−O2 = 2.0858(16), Sn−S1 = 2.8381(7), Sn−S2 = 2.9137(7), S1−P1 = 1.9798(9), S2−P2 = 1.9922(9).

phosphorus−tin coupling constants decrease from 865.4 Hz in **6** (a case of direct P−Sn bonding) to 114.4 Hz for **7** (geminal P═S−Sn bonding). The ^{119}Sn NMR chemical shift for **7** is −489 ppm. There is little information on the ^{119}Sn NMR chemical shifts for compounds structurally related to **7**. However, ^{119}Sn chemical shifts in the range −300 to −500 ppm were noted for dithiocarbamato compounds of five-coordinate tin.[12]

The structure of **7** was investigated by X-ray analysis (Figure 2).

The geometry about the tin atom in **7** is pyramidal, with the sulfur and oxygen atoms forming the base and the tin atom at the apex of a pyramid. The Sn−S bond lengths in **7** are 2.8381 and 2.9137 Å, which are relatively long according to a Cambridge Structural Database (CSD) search. Only one compound with a longer P═S−Sn bond (3.016 Å) than those in **7** has been structurally characterized.[13] The thiophosphoryl groups (−P═S) in **7** retain their double-bonded nature and are only slightly longer than, for example, the P═S bonds in P_2S_5 (1.96 Å).[14]

Oxidation of **6** by the addition of 30% hydrogen peroxide in water resulted in a fast reaction, yielding 2-(di-*tert*-butylphosphinoylmethyl)-1,1,1,3,3,3-hexafluoropropan-2-ol (**9**). The mechanism for the formation of **9** likely involves oxidation of the phosphorus atom of **6** and concomitant hydrolysis of the Sn−O bond. Further studies of the mechanism of this reaction have not been pursued. The oxidation of **6** by pyridine-*N*-oxide was a very slow process. Toluene solutions of **6** and pyridine-*N*-oxide did not react at the room temperature. Prolonged heating of the reaction mixture at 100 °C for 5 weeks resulted in two compounds being formed: the product of mono-oxidation, **10**, and complex **11**, with two phosphoryl groups (Scheme 5). The overall conversion of **6** to both products **10** and **11** was only about 20%.

The ^{31}P NMR spectrum of intermediate compound **10** consists of two doublets at 64.8 (phosphoryl group) and 19.9 ppm with the same phosphorus−phosphorus coupling constant ($^3J_{PP}$ = 18.7 Hz). The ^{31}P NMR spectrum of **11** consists of a singlet at 60.7 ppm with satellite couplings ($^2J_{P119Sn}$ = 96.33 Hz). Compound **10** was not isolated in pure form, and its assignment is tentative. Compound **11** was isolated by several recrystallizations from toluene, from which a crystal suitable for X-ray analysis was grown (Figure 3).

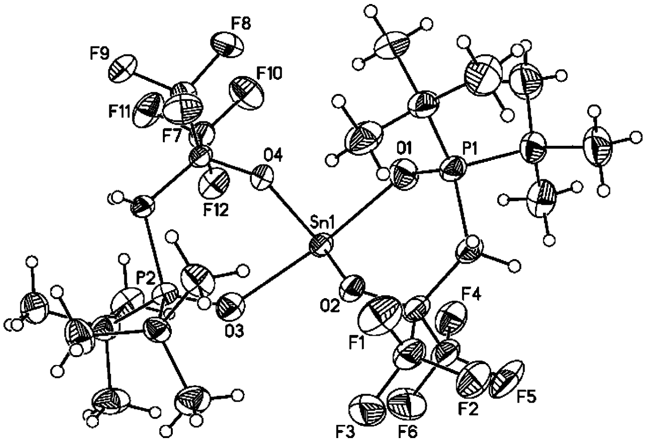

Figure 3. ORTEP drawing of tin(II), *trans*-bis[3-(di-*tert*-butylphosphinoyl)-1,1,1-trifluoro-2-(trifluoromethyl)-2-propanolato-*κO,κO*]-, **11**. Selected bond lengths (Å): Sn−O1 = 2.293(2), Sn−O2 = 2.0987(18), Sn−O3 = 2.298(2), Sn−O4 = 2.1051(17), O1−P1 = 1.502(2), O3−P2 = 1.490(2).

The formally divalent tin atom in **11** has a pyramidal geometry with four oxygen atoms at the base of the pyramid. The Sn−O(C) bonds in **11** are longer than in the sulfur analogue **7** (2.0987(18) and 2.1051(17) vs 2.0810(16) and 2.0858(16) Å). The (P═)O−Sn bonds (2.293(2) and 2.298(2) Å) in **11** are shorter than the (P═)S−Sn bonds in **7** (2.8381(7) and 2.9137(7) Å), and the additional ligand−ligand repulsions result in an elongation of the Sn−O(C) bonds. The phosphoryl groups (P═O) in **11**, like the thiophosphoryl groups (P═S) in **7**, remain double bonded at 1.502(2) and 1.490(2) Å. The Sn−O(═P) bond lengths in **11** are typical of double bonds.[15]

1-Azidoadamantane reacted with compound **6** at phosphorus. Only the monoadduct **12** was formed in this reaction (Scheme 6). Addition of a second molecule of 1-azidoadamantane did not take place even upon heating the reaction mixture at 100 °C for 2 weeks. The absence of any further reaction is likely due to the steric bulk created by the *tert*-butyl and adamantyl groups in **12**.

The ^{31}P NMR spectrum of **12** consists of two doublets at 12.50 and 59.60 ppm with the same phosphorus−phosphorus coupling constant ($^3J_{PP}$ = 12.90 Hz), but with two different satellite couplings.

The direct phosphorus−tin coupling constant was found to be 414.19 Hz, while the geminal P═N−Sn phosphorus−tin coupling constant was found to be less, 103.79 Hz. Complex **12** was structurally characterized by X-ray analysis (Figure 4). The P−Sn bond in **12** (3.228(4) Å) is the longest bond, among compounds with defined Sn−P bonds, in the Cambridge Structural Database. Nevertheless, the structural evidence suggests that a weak bond exists between the tin and phosphorus atoms of **12**. It should be noted that this bond is smaller by 0.77 Å than the sum of the van der Waals radii of phosphorus (1.80 Å) and tin (2.20 Å).[16] Overall, this P−Sn bond is on the border between a “defined” and “nonbonded interaction”.[17]

Compound **12** represents a rare instance of a complex between the phosphinimidate intermediate in the Staudinger reaction and

---

(11) Barney, A. A.; Heyduk, A. F.; Nocera, D. G. *Chem. Commun.* **1999**, 2379.

(12) Dakternieks, D.; Zhu, H.; Masi, D.; Mealli, C. *Inorg. Chem.* **1992**, *31*, 3601.

(13) Sekar, P.; Ibers, J. A. *Inorg. Chim. Acta* **2001**, *319*, 117.

(14) Haiduc, I.; Silvestru, C.; Roesky, H. W.; Schmidt, H.-G.; Noltemeyer, M. *Polyhedron* **1993**, *12*, 69.

(15) (a) Day, R. O.; Holmes, R. R.; Schmidpeter, A.; Stoll, K.; Howe, L. *Chem. Ber.* **1991**, *124*, 2443. (b) Mehring, M.; Löw, C.; Schürmann, M.; Uhlig, F.; Jurkschat, K.; Mahieu, B. *Organometallics* **2000**, *19*, 4613. (c) Reger, D. L.; Knox, S. J.; Lebioda, L. *Inorg. Chim. Acta* **1990**, *178*, 89.

Scheme 5

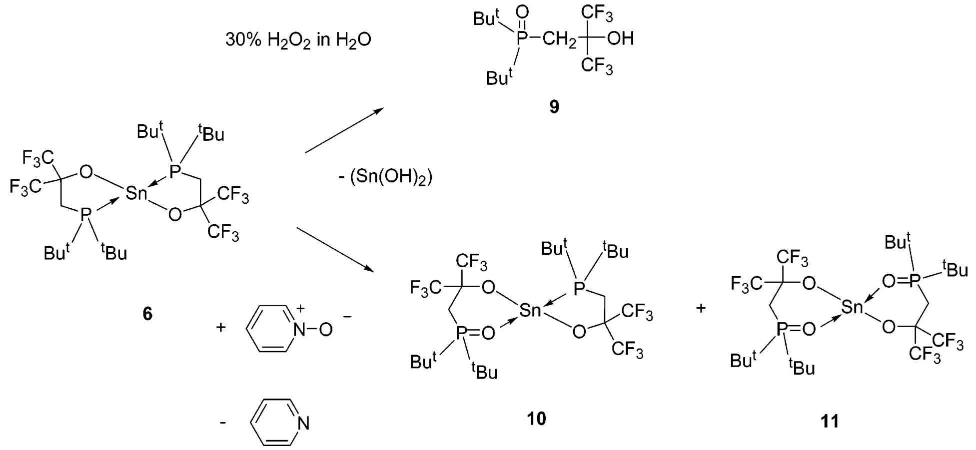

Scheme 6

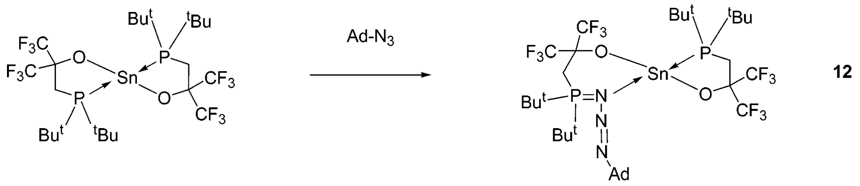

6

a metal. The decomposition of the phosphinimidate intermediate into iminophosphorane usually takes place through a triazo intermediate with a four-membered ring.[18] However, the linear phosphinimidate moiety in **12** is overcrowded by two *tert*-butyl and adamantyl groups, so it cannot close itself into a four-membered ring. The coordination of tin to the nitrogen atom of the iminophosphorane moiety probably also helps stabilize the phosphinimidate group. The stabilization of divalent germanium compounds by P^O ligand **1** is discussed below.

1.2. Synthesis, Reactivity, and Structural Studies of Divalent Germanium Compounds. The reaction between the lithium salt of 2-[(di-*tert*-butylphosphino)methyl]-1,1,1,3,3,3-hexafluoropropan-2-ol (**13**) and the germanium(II) chloride complex of 1,4-dioxane was used to prepare divalent germanium compound **14** supported by two P^O chelating five-membered rings (Scheme 7).

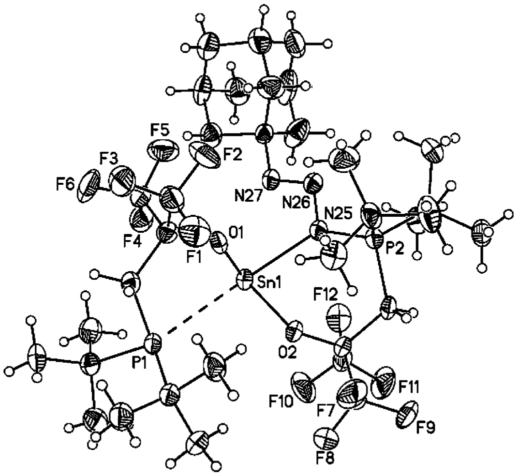

Figure 4. ORTEP drawing of tin(II), *trans*-[3-(di-*tert*-butylphosphino)-1,1,1-trifluoro-2-(trifluoromethyl)-2-propanolato-*O,P*], [3-(*P,P*-di-*tert*-butyl-*N*-(diazoadamantyl)phosphinimyl)-1,1,1-trifluoro-2-(trifluoromethyl)-2-propanolato-*κO,κN*]-, **12**. Selected bond lengths (Å): Sn−O1 = 2.098(4), Sn−O2 = 2.134(3), Sn−N25 = 2.330(4), Sn−P1 = 3.228(4).

Scheme 7

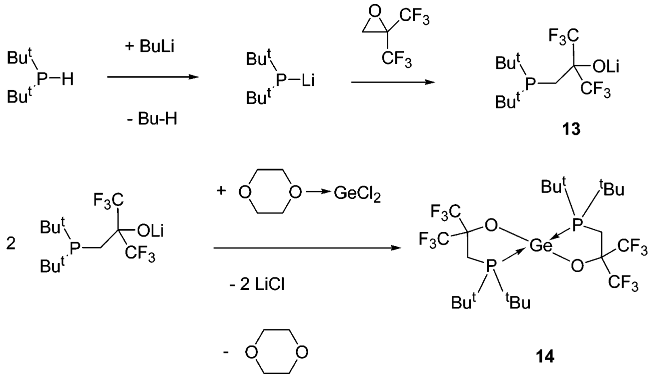

The ^{31}P NMR resonance of **14** is observed at 15.2 ppm. As was noted earlier for the tin analogues **6**, the chemical shifts of the phosphorus atoms are not shifted significantly downfield relative to the starting phosphine. Again, this is likely an indication of weak coordination.

The structure of compound **14** was investigated by X-ray analysis (Table 1 and Figure 5). The germanium atom in **14** is situated at the apex of a square pyramid, with the two phosphorus and two oxygen atoms forming the base. The shorter Ge−O bonds in **14**, relative to the Sn−O bonds in **6** (Table 1), result in an increase in ligand−ligand repulsion, which in turn produces a larger P−Ge−P bond angle, 153.8°, compared with the P−Sn−P angle (136.4°). The Ge−P bond lengths in **14** are 2.7331(12) and 2.7585(12) Å, which are long. There is only structurally characterized complex in the Cambridge Structural Database with longer Ge−P bonds than those in **14**.[19]

---

(16) Batsanov, S. S. *THEOCHEM* **1999**, *468*, 151.

(17) (a) Chen, T.; Duesler, E. N.; Paine, R. T.; Noth, H. *Inorg. Chem.* **1997**, *36*, 1070. (b) Hoppe, S.; Weichmann, H.; Jurkschat, K.; Schneider-Koglin, C.; Drager, M. *J. Organomet. Chem.* **1996**, *505*, 63. (c) Lee, T.; Lee, S. W.; Jang, H. G.; Kang, S. O.; Ko, J. *Organometallics* **2001**, *20*, 741.

(18) Quin, L. D. *A Guide to Organophosphorus Chemistry*; John Wiley & Sons: New York, 2000.

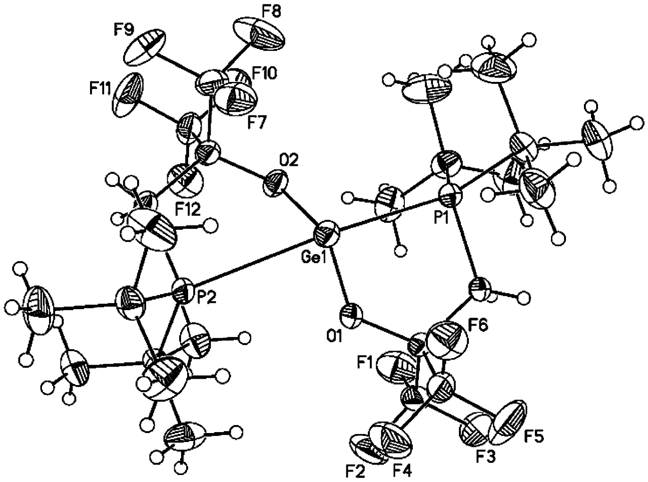

Figure 5. ORTEP drawing of germanium(II), *trans*-bis[3-(di-*tert*-butylphosphino)-1,1,1-trifluoro-2-(trifluoromethyl)-2-propanolato-*O,P*]-, **14**. A crystal was grown from pentane.

The divalent, electron-rich compound **14** can react with oxidizing reagents on two phosphorus atoms (due to very weak Ge$-$P bonds) with or without engaging the germanium center. Our expectation was that the divalent germanium in **14** would be more prone to oxidation reaction than the tin analogue **6**. In general, divalent germanium compounds are more reactive than divalent tin compounds.[5] The reaction of 1-azidoadamantane with compound **14** was carried out. The reaction did not take place at room temperature: only prolonged heating for 5 weeks resulted in full conversion of the starting complex (Scheme 8).

In contrast to the tin analogue **6**, the Staudinger phosphinimidate intermediate **15** was not isolated. Most likely this is because of the greater steric crowding in intermediate **15** than in **12**, which results in radical decomposition of **15**. The reaction was not a selective one. Three major products were separated by sequential crystallizations and chromatography. Compound **16** was obtained in 39% yield, and it was the major product isolated from the reaction. It contains two different phosphorus atoms in penta- and trivalent states and tetravalent germanium. We speculate that the mechanism of formation of **16** perhaps involves decomposition of the triazo moiety of **15** with elimination of dinitrogen and adamantyl radical from the P^N chelating ligand[20] and elimination of *tert*-butyl radical or isobutene and hydrogen from the P^O ligand.[21]

The ^{31}P NMR spectrum of **16** consists of two singlets: an upfield signal characteristic of germanylphosphines[22] at -69.99 ppm (Ge$-$P) and a downfield signal at 42.27 ppm (Ge$-$N$=$P) in a ratio 1:1. The ORTEP drawing of **16** is shown in Figure 6.

There is a change in Ge$-$O bond lengths on moving from divalent to tetravalent germanium: the Ge$-$O bond lengths in divalent **14** (1.91 Å) are longer than in tetravalent **16** (1.82 Å). The iminophosphoryl groups ($-$P$=$N$-$Ge) in **16** evidently do not exhibit "betaine-like" bonding, i.e., Ge$=$N$-$P$-$. The P$=$N bond is quite short and characteristic of a double bond [1.576(4) Å]. The germanium atom in **16** has a tetrahedral geometry.

The mode of the decomposition of the triazo moiety in **15** with the elimination of dinitrogen and a shift of the adamantyl radical from the P^N chelating ligand to germanium explains the formation of half a molecule of **17**. The formation of the Ge$-$O$-$Ge bridge in **17** may result from degradation of the parent P^O ligand. It should be noted that the Ge$-$O$-$Ge fragment in **17** is very linear, with an angle of 177.4° (Figure 7).

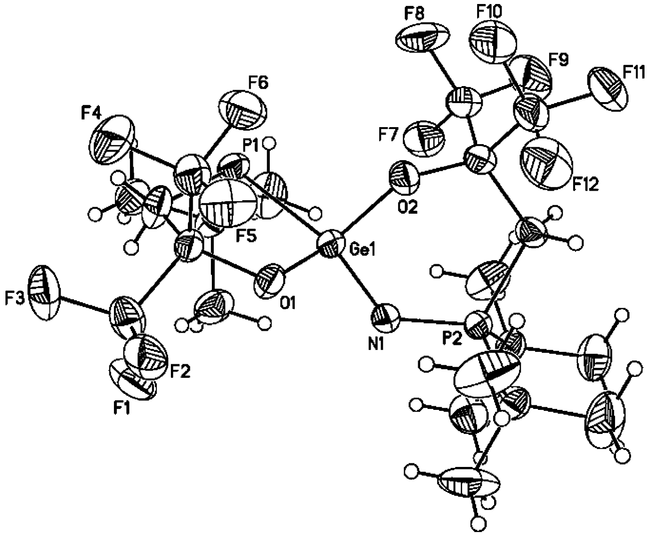

Figure 6. ORTEP drawing of germanium(IV), *trans*-[3-(*tert*-butylphosphino)-1,1,1-trifluoro-2-(trifluoromethyl)-2-propanolato-*κO,κP*], [3-(*P,P*-di-*tert*-butylphosphinimyl)-1,1,1-trifluoro-2-(trifluoromethyl)-2-propanolato-*κO,κN*]-, **16**. A crystal was grown from pentane. Selected bond lengths (Å): Ge$-$O1 $=$ 1.817(3), Ge$-$O2 $=$ 1.820(4), Ge$-$N1 $=$ 1.753(4), Ge$-$P1 $=$ 2.2988(15), N1$-$P2 $=$ 1.576(4).

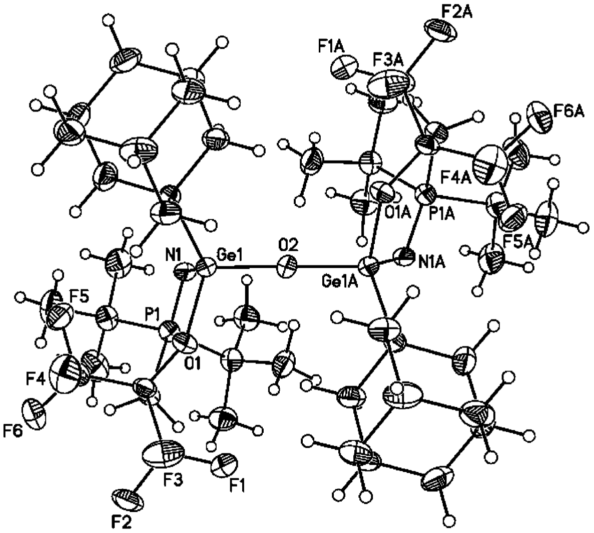

Figure 7. ORTEP drawing of oxo-bis[adamantyl[3-(*P,P*-di-*tert*-butylphosphinimyl)-1,1,1-trifluoro-2-(trifluoromethyl)-2-propanolato-*κO,κN*]germanium(IV)], **17**. Selected bond lengths (Å): Ge1$-$O2 $=$ 1.7304(5), Ge1$-$O1 $=$ 1.820(2), Ge$-$N1 $=$ 1.745(3), N1$-$P1$=$ 1.565(3). Angle of Ge1$-$O2$-$Ge1A is 177.4(2)°.

The Ge$-$O distances in the Ge$-$O$-$Ge bridge (1.73 Å) are significantly shorter than those in the O^N chelating rings (1.82 Å). The same short Ge$-$O distance of 1.73 Å is found in only one other known linear oxobisgermane, Bz$_3$Ge$-$O$-$GeBz$_3$.[23] It has been suggested that the linearity of R$_3$Ge$-$O$-$GeR$_3$ compounds increases when R is an electron donor, particularly an amide.[23b] While the shortenening of Ge$-$O bonds and

---

(19) Karsch, H. H.; Deubelly, B.; Hanika, G.; Riede, J.; Müller, G. *J. Organomet. Chem.* **1988**, *344*, 153.

(20) (a) Alajarin, M.; Vidal, A.; Ortin, M.-M.; Bautista, D. *New J. Chem.* **2004**, *28*, 570. (b) Seibert, W. *Chem. Ber.* **1948**, *81*, 266.

(21) (a) Li, S. H.; Buchan, N. I.; Larsen, C. A.; Stringfellow, G. B. *J. Cryst. Growth* **1989**, *98*, 309. (b) Murugesan, R.; Subramanian, S. *Mol. Phys.* **1979**, *38*, 1941.

(22) Schumann, H.; Kroth, H. J. *Z. Naturforsch., B*: *Anorg. Chem., Org. Chem.* **1977**, *32B*, 513.

(23) (a) Glidwell, C.; Lilies, D. C. *J. Organomet. Chem.* **1979**, *174*, 275. (b) Livant, P.; Northcott, J.; Webb, T. R. *J. Organomet. Chem.* **2001**, *620*, 133.

Scheme 8

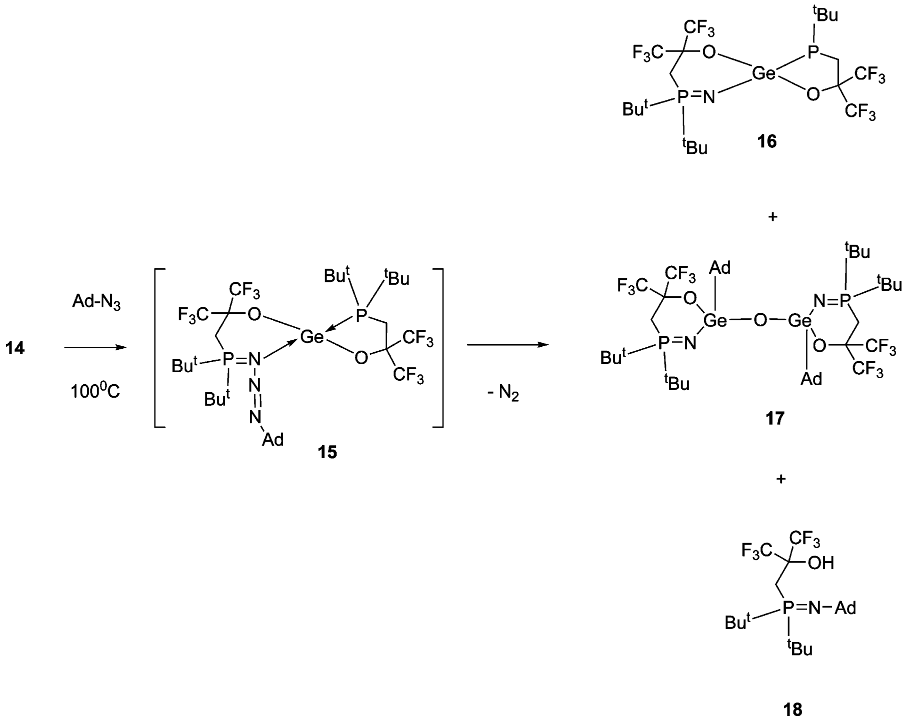

Scheme 9

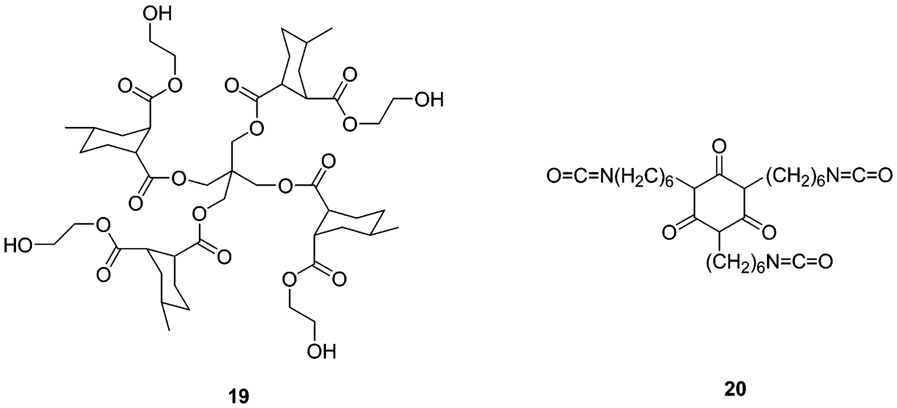

linearity of the Ge−O−Ge bridge may be explained by the existence of $d_\pi - p_\pi$ bonding interactions between germanium and oxygen, a perhaps better explanation makes use of the ligand close-packing (LCP) model and takes into consideration the importance of ligand−ligand repulsions in molecular geometry and bond lengths.[24] According to this model, when two sterically bulky germanium ligands coordinate to more electronegative oxygen atoms, ligand−ligand repulsions dominate, giving rise to a linear Ge−O−Ge bridge. Packing does not restrict the two sterically bulky germanium groups in the linear geometry of **17**, and as a result the shorter Ge−O bonds in the Ge−O−Ge bridge are observed.

The iminophosphine **18** is an expected product of the Staudinger reaction between the ligand in starting compound **14** and 1-azidoadamantane. It seems to be formed in one of the degradation pathways of intermediate **15**.

2. Divalent Tin and Germanium Compounds as Catalysts for the Formation of Polyurethanes. Organometallics of the group 14 elements, particularly dibutyltin derivatives, are known to catalyze transesterification, transcarbamoylation, and urethane formation.[25] The production of polyurethanes is usually achieved by the cross-linking reaction of oligomeric polyols and polyisocyanates. Typical examples are shown in Scheme 9.[26]

The usual catalysts for this process are dibutyltindilaurate and tertiary amines. Dialkyl and trialkyltin derivatives have toxicity issues,[27] and the search for less toxic catalysts is an important task. Thus, the novel divalent tin compounds **6**, **7**, and **12**, without alkyl−tin bonds, and divalent germanium compound **14** were tested as the catalysts for polyurethane formation.

“Gel time” was measured under both anaerobic conditions (under nitrogen) and aerobic conditions. The “gel time” corresponds to the time in hours following activation at which flow is no longer observed in a coating mixture.[28] The results of the application of novel divalent tin and germanium compounds in the catalytic formation of polyurethanes are shown in Table 2.

---

(24) Gillespie, R. J. *Coord. Chem. Rev.* **2000**, *197*, 51.

(25) Hostettler, F.; Cox, E. F. *Ind. Eng. Chem.* **1960**, *52*, 609.

(26) Wicks, Z. W.; Jones, F. N.; Pappas, S. P. *Organic Coatings: Science and Technology*; Wiley: New York, 1992; p 204.

(27) (a) Boyer, I. J. *Toxicology* **1989**, *55*, 253. (b) Lytle, T. F.; Manning, C. S.; Walker, W. W.; Lytle, J. S.; Page, D. S. *Appl. Organomet. Chem.* **2003**, *17*, 653.

(28) Bernard, J.-M.; Frances, J.-M.; Jousseaume, B.; Noiret, N.; Pereyre, M. PCT Int. Appl., 1995, 37 pp, WO 9521694 A1 19950817.

Table 2. Gel Times under Nitrogen and under Air for Compounds 1, 6, 7, 12, and 14 in the Formation of Polyurethanes

entry	compound	concentration (ppm)	time to gel under nitrogen (h)	time to gel under air (h)
1	**6**	1500	1.9	1.6
2	**6**	700	2.6	2.3
3	**6**	500	3.2	3.1
4	**6**	250	6.2	5.7
5	**7**	1800	1.5	1.0
6	**7**	1000	2.6	2.0
7	**12**	5000	11.0	11.0
8	**12**	500	19.0	19.0
9	**14**	4000	38.0	7.9
10	**1**	1800	72.0	72.0
11	no catalyst	N/A	72.0	72.0

The divalent tin compounds **6** and **7** were found to be efficient catalysts for polyurethane formation (entries 1−6 in Table 2). The gel times decreased with increasing catalyst loading, as expected. A mild latency effect[28] was found for the case of compound **7**. Polymerization samples exposed to air have shorter gel times than ones kept under nitrogen (entries 5 and 6). The divalent tin adduct **12**, with a bulky adamantyl phosphinimidate moiety, was the least active among tested tin compounds. The decreased catalyst activity of **12** is likely caused by additional steric blocking of the tin center compared with compound **6**.

The divalent germanium compound **14** was active in polyurethane formation, but was an order of magnitude less active than corresponding tin analogue **6**. For compound **14** (Table 2, entry 9), the gel time under air was 5 times faster than that under nitrogen. The ligand **1** itself did not have an impact on the polymerization rates (entries 10 and 11).

In conclusion, the application of a new P^O chelating phosphine **1** with a sterically bulky “soft” di-*tert*-butyl phosphine center and sterically bulky “hard” fluorinated alkoxy center resulted in the stabilization of monomeric divalent compounds of tin (**6**) and germanium (**14**). Experiments directed toward the stabilization of unusual coordination states of elements other than iridium, tin, and germanium by phosphine **1** and its phosphoryl, thiophosphoryl, and iminophosphoryl derivatives are underway in our laboratory.

Experimental Section

All air-sensitive compounds were prepared and handled under a N_2/Ar atmosphere using standard Schlenk and inert-atmosphere box techniques. Anhydrous solvents were used in the reactions. Solvents were distilled from drying agents or passed through columns under an argon or nitrogen atmosphere. 1-Azidoadamantane, sulfur, bis[bis(trimethylsilyl)amino]tin(II), germanium(II) chloride dioxane complex (1:1), and toluene were purchased from Aldrich. The polyol **19** is manufactured by DuPont Performance Coatings. The polyisocyanate **20** is commercially available from Bayer under the trademark Desmodur 3300. The melting points were measured by DSC.

Tin(II), *trans*-bis[3-(di-*tert*-butylphosphino)-1,1,1-trifluoro-2-(trifluoromethyl)-2-propanolato-*O*,*P*]- (6). A 15.62 g sample (0.048 mol) of 2-[(di-*tert*-butylphosphino)methyl]-1,1,1,3,3,3-hexafluoropropan-2-ol (**1**) was dissolved in 200 mL of toluene. Then 9.5 g (0.022 mol) of bis[bis(trimethylsilyl)amino]tin(II) was added dropwise to the above solution. The reaction mixture was stirred for 24 h, and the solvent and formed bis(trimethylsilyl)amine were removed in vacuo at 1 mmHg. The residue was recrystallized from 50 mL of pentane at −30 °C. Yield of tin(II), *trans*-bis[3-(di-*tert*-butylphosphino)-1,1,1-trifluoro-2-(trifluoromethyl)-2-propanolato-*O*,*P*]− (**6**) was 12.71 g (76%) as a white solid with mp 207.6 °C (dec). ^{1}H NMR (500 MHz, C_6D_6, TMS): δ 1.00 (s, 36 H, Me), 2.10 (s, 4 H, CH_2). ^{19}F NMR (500 MHz, Tol-D_8): δ −76.85 (s, 12F). ^{31}P NMR (500 MHz, Tol-D_8): δ 18.2 ($^1J_{P119Sn}$ = 865.36 Hz, $^1J_{P117Sn}$ = 827.18 Hz). ^{119}Sn NMR (400 MHz, C_6D_6, Me_4Sn): δ −292 (br, 1Sn). Anal. Calcd for $C_{24}H_{40}F_{12}O_2P_2Sn$ (mol wt 769.21): C, 37.47; H, 5.24. Found: C, 37.54; H, 5.27. The structure was proven by X-ray analysis.

Tin(II), *trans*-bis[3-(di-*tert*-butylphosphinothioyl)-1,1,1-trifluoro-2-(trifluoromethyl)-2-propanolato-*κO*,*κS*]- (7). A 3.0 g (0.0039 mol) sample of tin(II), *trans*-bis[3-(di-*tert*-butylphosphino)-1,1,1-trifluoro-2-(trifluoromethyl)-2-propanolato-*O*,*P*]- (**6**) and 0.27 g (0.0086 mol) of sulfur were stirred in 200 mL of toluene at room temperature for 48 h. The solvent was removed in vacuo at 1 mmHg, and the residue was recrystallized from 50 mL of pentane. Yield of tin(II), *trans*-bis[3-(di-*tert*-butylphosphinothioyl)-1,1,1-trifluoro-2-(trifluoromethyl)-2-propanolato-*κO*,*κS*]- (**7**) was 3.14 g (97%) as a white solid with mp 204.5 °C (dec). ^{1}H NMR (500 MHz, C_6D_6, TMS): δ 1.00 (s, 36 H, Me), 2.30 (s, 4 H, CH_2). ^{19}F NMR (500 MHz, C_6D_6): δ −76.30 (s, 12F). ^{31}P NMR (500 MHz, THF-D_8): δ 67.11 ($^2J_{P119Sn}$ = 114.4 Hz). ^{119}Sn NMR (400 MHz, THF-D_8, Me_4Sn): δ −489 (br, 1Sn). Anal. Calcd for $C_{24}H_{40}F_{12}O_2P_2S_2Sn$ (mol wt 833.34): C, 34.59; H, 4.84. Found: C, 34.72; H, 5.03. The structure was proven by X-ray analysis.

2-(Di-*tert*-butylphosphinoylmethyl)-1,1,1,3,3,3-hexafluoropropan-2-ol (9). A 1.0 g (0.0013 mol) sample of tin(II), *trans*-bis[3-(di-*tert*-butylphosphino)-1,1,1-trifluoro-2-(trifluoromethyl)-2-propanolato-*O*,*P*]- (**6**) was dissolved in 50 mL of methylene chloride. Then 1.0 g of a 30% solution of hydrogen peroxide was added to the above solution. After 1 h, the organic phase was separated and dried over magnesium sulfate overnight. The solvent was removed in vacuo at 1 mmHg, and the residue was recrystallized from 10 mL of pentane. Yield of 2-(di-*tert*-butylphosphinoylmethyl)-1,1,1,3,3,3-hexafluoropropan-2-ol]- (**9**) was 0.71 g (80%) as a white solid with mp 87.5 °C (with sublimation). ^{1}H NMR (500 MHz, THF-D_8, TMS): δ 1.12 (d, $^3J_{P,H}$ = 13.4 Hz, 18 H, Me), 2.30 (d, $^3J_{P,H}$ = 3.7 Hz, 2 H, CH_2). ^{19}F NMR (500 MHz, THF-D_8): δ −81.20 (s, 12F). ^{31}P NMR (500 MHz, THF-D_8): δ 64.95 (s, 1P). Anal. Calcd for $C_{12}H_{21}F_6O_2P$ (mol wt 342.26): C, 42.11; H, 6.18; P, 9.05. Found: C, 42.25; H, 6.22; P, 9.13. The structure was proven by X-ray analysis.

Reaction of Pyridine-*N*-oxide and 2. A 3.0 g (0.0039 mol) sample of tin(II), *trans*-bis[3-(di-*tert*-butylphosphino)-1,1,1-trifluoro-2-(trifluoromethyl)-2-propanolato-*O*,*P*]- (**6**) and 4.05 g (0.043 mol) of pyridine-*N*-oxide were stirred in 200 mL of toluene at 100 °C for 5 weeks. According to ^{31}P NMR 20% of the starting compound was consumed to give two new signals (compounds **10** and **11**) in about 2:1 ratio. Tin(II), *trans*-[3-(di-*tert*-butylphosphino)-1,1,1-trifluoro-2-(trifluoromethyl)-2-propanolato-*O*,*P*], [3-(di-*tert*-butylphosphinoyl)-1,1,1-trifluoro-2-(trifluoromethyl)-2-propanolato-*κO*,*κO*]- (**10**) has the following chemical shifts. ^{31}P NMR (500 MHz, THF-D_8): δ 64.8 (d, $^3J_{PP}$ = 18.7 Hz, $^2J_{P119Sn}$ = 118.9 Hz, 1P, P=O), 19.9 (d, $^3J_{PP}$ = 18.7 Hz, $^1J_{P119Sn}$ = 270.8 Hz, 1P). The solvent was removed in vacuo at 1 mmHg, and the residue was recrystallized from 20 mL of pentane five times. Yield of tin(II), *trans*-bis[3-(di-*tert*-butylphosphinoyl)-1,1,1-trifluoro-2-(trifluoromethyl)-2-propanolato-*κO*,*κO*]- (**11**) was 0.19 g (6%) as a white solid with mp 103.5 °C (with sublimation). ^{1}H NMR (500 MHz, Tol-D_8, TMS): δ 1.10 (s, 36 H, Me), 2.25 (s, 4 H, CH_2). ^{31}P NMR (500 MHz, Tol-D_8): δ 60.7 ($^2J_{P119Sn}$ = 96.33 Hz). Anal. Calcd for $C_{24}H_{40}F_{12}O_4P_2Sn$ (mol wt 801.21): C, 3.98; H, 5.03; P, 7.73. Found: C, 4.10; H, 5.08; P, 7.84. The structure was proven by X-ray analysis.

Tin(II), *trans*-[3-(di-*tert*-butylphosphino)-1,1,1-trifluoro-2-(trifluoromethyl)-2-propanolato-*O*,*P*], [3-(*P*,*P*-di-*tert*-butyl-*N*-(diazoadamantyl)phosphinimyl)-1,1,1-trifluoro-2-(trifluoromethyl)-2-propanolato-*κO*,*κN*]- (12). A 3.0 g (0.0039 mol) sample of tin-

Table 3. Summary of Crystal Data, Data Collection, and Structural Refinement Parameters for 6, 7, 9, 11, and 12

	6	**7**	**9**	**11**	**12**
empirical formula	$C_{24}H_{40}F_{12}O_2P_2Sn$	$C_{24}H_{40}F_{12}O_2P_2$ S_2 Sn	$C_{12}H_{21}F_6O_2P$	$C_{27.5}H_{40}F_{12}O_4P_2Sn$	$C_{34}H_{55}F_{12}N_3$-O_2P_2Sn
fw	769.19	833.31	342.26	843.22	946.44
cryst color, form	colorless, irreg block	colorless, plate	colorless, block	colorless, rect plate	colorless, rect block
cryst syst	triclinic	monoclinic	monoclinic	monoclinic	triclinic
space group	$P\bar{1}$	$C2/c$	$P2(1)/c$	$P2(1)/c$	$P\bar{1}$
a (Å)	10.976(4)	29.6783(15)	18.8933(7)	21.039(3)	10.4018(18)
b (Å)	16.162(4)	11.4441(6)	15.6929(16)	9.5275(16)	11.635(2)
c (Å)	19.627(4)	20.1419(10)	10.9181(17)	17.940(3)	17.737(3)
α (deg)	71.845(8)	90	90	90	81.550(2)
β (deg)	89.785(8)	95.6190(10)	104.105(4)	92.505(2)	77.711(2)
γ (deg)	77.397(8)	90	90	90	81.393(2)
V ($Å^3$)	3220.9(16)	6808.2(6)	3139.5(6)	3592.6(10)	2059.2(6)
Z	4	8	8	4	2
density (g/cm^3)	1.586	1.626	1.448	1.559	1.526
abs *μ* (mm^{-1})	0.983	1.055	0.238	0.893	0.786
F(000)	1552	3360	1424	1700	968
cryst size (mm)	0.50 × 0.47 × 0.45	0.42 × 0.42 × 0.04	0.15 × 0.14 × 0.02	0.50 × 0.36 × 0.08	0.31 × 0.22 × 0.08
temp (°C)	−100	−100	−100	−100	−100
scan mode	*ω*	*ω*	*ω*	*ω*	*ω*
detector	Bruker-CCD	Bruker-CCD	Raxis-Image Plate	Bruker-CCD	Bruker-CCD
θ_{max} (deg)	28.42	28.56	24.11	28.5	26.3
no. obsd reflns	23 573	35 660	13 583	33 939	19 059
no. uniq reflns	15 685	8601	4485	9051	8288
R_{merge}	0.022	0.0477	0.0676	0.0394	0.0798
no. params	765	400	400	445	499
S^b	1.051	1.049	1.076	0.948	0.985
R indices [$I > 2\sigma(I)$]^a	$wR_2 = 0.142$, $R_1 = 0.052$	$wR_2 = 0.073$, $R_1 = 0.034$	$wR_2 = 0.138$, $R_1 = 0.058$	$wR_2 = 0.083$, $R_1 = 0.035$	$wR_2 = 0.123$, $R_1 = 0.057$
R indices (all data)^a	$wR_2 = 0.151$, $R_1 = 0.065$	$wR_2 = 0.080$, $R_1 = 0.051$	$wR_2 = 0.150$, $R_1 = 0.092$	$wR_2 = 0.092$, $R_1 = 0.050$	$wR_2 = 0.144$, $R_1 = 0.102$
max. diff peak, hole (e/$Å^3$)	5.982, −1.660	0.565, −0.890	0.602, −0.310	1.421, −0.788	0.867, −1.275

*$R_1 = \sum ||F_o| - |F_c|| / \sum |F_o|$, $wR_2 = \{\sum[w(F_o^2 - F_c^2)^2] / \sum[w(F_o^2)^2]\}^{1/2}$ (sometimes denoted as R_w^2). ^{b} GooF $= S = \{\sum[w(F_o^2 - F_c^2)^2]/(n - p)\}^{1/2}$, where *n* is the number of reflections, and *p* is the total number of refined parameters.

(II), *trans*-bis[3-(di-*tert*-butylphosphino)-1,1,1-trifluoro-2-(trifluoromethyl)-2-propanolato-*O*,*P*]- (**6**) and 0.63 g (0.0041 mol) of 1-azidoadamantane were stirred in 200 mL of toluene at room temperature for 5 days. The solvent was removed in vacuo at 1 mmHg, and the residue was recrystallized from 50 mL of pentane. Yield of tin(II), *trans*-[3-(di-*tert*-butylphosphino)-1,1,1-trifluoro-2-(trifluoromethyl)-2-propanolato-*O*,*P*], [3-(*P*,*P*-di-*tert*-butyl-*N*-(diazoadamantyl)phosphinimyl)-1,1,1-trifluoro-2-(trifluoromethyl)-2-propanolato-*κO*,*κN*]- (**12**) was 3.20 g (87%) as a slightly yellow solid with mp 167.7 °C (dec). ^{1}H NMR (500 MHz, C_6D_6, TMS): δ 1.05 (d, $^3J_{P,H} = 13.8$ Hz, 9 H, Me), 1.16 (d, $^3J_{P,H} = 13.8$ Hz, 9 H, Me), 1.20 (d, $^3J_{P,H} = 14.7$ Hz, 9 H, Me), 1.35 (d, $^3J_{P,H} = 14.4$ Hz, 9 H, Me), 1.63 (m, 6 H, Adamantyl), 1.90 (m, 6 H, Adamantyl), 2.05 (m, 3 H, Adamantyl), 2.40 (m, 2 H, P−CH_2), 2.30 (m, 2 H, P−CH_2). ^{19}F NMR (500 MHz, C_6D_6): δ −74.55 (m, 3F), −74.87 (m, 3F), −76.24 (m, 3F), −77.82 (m, 3F). ^{31}P NMR (500 MHz, Tol-D_8): δ 12.50 (d, $^2J_{PP} = 12.90$ Hz, $^1J_{P119Sn} = 414.19$ Hz, 1P), 59.60 (d, $^2J_{PP} = 12.90$ Hz, $^2J_{P119Sn} = 103.79$ Hz, 1P). ^{119}Sn NMR (400 MHz, THF-D_8, Me_4Sn): δ −488 (br, 1Sn). Anal. Calcd for $C_{34}H_{55}F_{12}N_3O_2P_2Sn$ (mol wt 946.47): C, 43.15; H, 5.86; N, 4.44. Found: C, 43.26; H, 6.01; N, 4.63. The structure was proven by X-ray analysis.

Germanium(II), *trans*-bis[3-(di-*tert*-butylphosphino)-1,1,1-trifluoro-2-(trifluoromethyl)-2-propanolato-*O*,*P*]- (14). A 14.45 g (0.095 mol) sample of lithium di-*tert*-butylphosphide, 18.81 g (0.105 mol) of 2,2-bis(trifluoromethyl)oxirane, and 80 mL of THF were stirred at room temperature for 1 h. Then 10.0 g (0.043 mol) of germanium(II) chloride dioxane complex (1:1) was added in one portion to the reaction mixture. The reaction mixture was stirred for 24 h, and the solvent was removed in vacuo at 1 mmHg. The residue was redissolved in 100 mL of pentane. The LiCl was filtered off, and the final product was purified by the recrystallizion from 50 mL of pentane at −30 °C. Yield of germanium(II), *trans*-bis[3-(di-*tert*-butylphosphino)-1,1,1-trifluoro-2-(trifluoromethyl)-2-propanolato-*O*,*P*]- (**14**) was 14.3 g (46%) as a white solid with mp 186.2 °C (dec). ^{1}H NMR (500 MHz, THF-D_8, TMS): δ 1.30 (s, 36 H, Me), 2.35 (s, 4 H, CH_2).^{19}F NMR (500 MHz, THF-D_8): δ −76.58 (s, 12F). ^{31}P NMR (500 MHz, THF-D_8): δ 15.2 (s, 1P). Anal. Calcd for $C_{24}H_{40}F_{12}O_2GeP_2$ (mol wt 723.14): C, 39.86; H, 5.58. Found: C, 40.03; H, 6.17. The structure was proven by X-ray analysis.

Reaction of 1-Azidoadamantane with Germanium(II), *trans*-bis[3-(di-*tert*-butylphosphino)-1,1,1-trifluoro-2-(trifluoromethyl)-2-propanolato-*O*,*P*]- (14). Germanium(IV), *trans*-[3-(*tert*-butylphosphino)-1,1,1-trifluoro-2-(trifluoromethyl)-2-propanolato-*κO*,*κP*], [3-(*P*,*P*-di-*tert*-butylphosphinimyl)-1,1,1-trifluoro-2-(trifluoromethyl)-2-propanolato-*κO*,*κN*]- (16). A 3.0 g (0.0042 mol) sample of germanium(II), *trans*-bis[3-(di-*tert*-butylphosphino)-1,1,1-trifluoro-2-(trifluoromethyl)-2-propanolato-*O*,*P*]- (**14**) and 1.6 g (0.0090 mol) of 1-azidoadamantane were stirred in 600 mL of toluene at 100 °C for 5 days. The solvent was removed in vacuo at 1 mmHg, and the residue was recrystallized from 50 mL of pentane. The first crop of the crystals was germanium(IV), *trans*-[3-(*tert*-butylphosphino)-1,1,1-trifluoro-2-(trifluoromethyl)-2-propanolato-*κO*,*κP*], [3-(*P*,*P*-di-*tert*-butylphosphinimyl)-1,1,1-trifluoro-2-(trifluoromethyl)-2-propanolato- *κO*,*κN*]-, **16**. Yield of compound **16** was 1.10 g (39%) as a white solid with mp 83.7 °C (dec). ^{1}H NMR (500 MHz, C_6D_6, TMS): δ 1.20 (d, $^3J_{P,H} = 13.7$ Hz, 9 H, Me), 1.25 (d, $^3J_{P,H} = 13.6$ Hz, 9 H, Me), 1.29 (d, $^3J_{P,H} = 14.0$ Hz, 9 H, Me), 1.34 (d, $^3J_{P,H} = 14.1$ Hz, 9 H, Me), 2.40 (m, 2 H, P−CH_2), 2.70 (m, 2 H, P−CH_2). ^{19}F NMR (500 MHz, C_6D_6): δ −77.25 (m, 3F), −80.57 (m, 3F), −81.00 (m, 3F), −82.93 (m, 3F). ^{31}P NMR (500 MHz, THF-D_8): δ − 69.99 (s, 1P), 42.27 (s, 1P). Anal. Calcd for $C_{20}H_{31}F_{12}GeNO_2P_2$ (mol wt 680.03): C, 35.32; H, 4.59; N, 2.06. Found: C, 35.37; H, 4.73; N, 2.30. The structure was proven by X-ray analysis. The second crop was oxo-bis[adamantyl-[3-(*P*,*P*-di-*tert*-butylphosphinimyl)-1,1,1-trifluoro-2-(trifluoromethyl)-2-propanolato-*κO*,*κN*]germanium(IV)], **17**. Yield of compound

Table 4. Summary of Crystal Data, Data Collection, and Structural Refinement Parameters for 14, 16, 17, and 18

	14	**16**	**17**	**18**
empirical formula	$C_{24}H_{40}F_{12}GeO_2P_2$	$C_{20}H_{31}F_{12}GeNO_2P_2$	$C_{24.5}H_{41}F_6GeNO_{1.5}P$	$C_{22}H_{36}F_6NOP$
fw	723.09	679.99	591.14	475.49
cryst color, form	colorless, trapezoidal block	colorless, irreg block	colorless, plate	colorless, block
cryst syst	triclinic	monoclinic	monoclinic	monoclinic
space group	$P\bar{1}$	$P2(1)/c$	$C2/c$	$P2(1)/c$
a (Å)	10.7537(10)	14.454(2)	25.888(5)	8.5623(13)
b (Å)	16.0182(15)	9.5410(17)	9.7436(19)	16.439(3)
c (Å)	19.8424(18)	20.829(4)	21.499(4)	16.930(3)
α (deg)	71.3300(10)	90	90.00(3)	90
β (deg)	89.796(2)	107.053(4)	108.26(3)	98.101(2)
γ (deg)	80.542(2)	90	90.00(3)	90
V (Å^3)	3189.7(5)	2746.1(8)	5149.9(18)	2359.1(6)
Z	4	4	8	4
density (g/cm^3)	1.506	1.645	1.525	1.339
abs μ (mm^{-1})	1.152	1.333	1.316	0.177
F(000)	1480	1376	2464	1008
cryst size (mm)	0.50 × 0.24 × 0.16	0.14 × 0.05 × 0.02	0.22 × 0.08 × 0.02	0.50 × 0.48 × 0.45
temp (°C)	−100	−100	−100	−100
scan mode	ω	ω	ω	ω
detector	Bruker-CCD	Bruker-CCD	Bruker-CCD	Bruker-CCD
θ_{max} (deg)	28.49	26.42	27.42	28.54
no. obsd reflns	27 903	16 702	18 024	22 814
no. uniq reflns	15 912	5597	7803	5985
R_{merge}	0.0323	0.0953	0.0950	0.0457
no. params	764	369	329	372
S^b	1.016	0.963	0.898	1.035
R indices [$I > 2\sigma(I)$]^a	$wR_2 = 0.165$, $R_1 = 0.060$	$wR_2 = 0.119$, $R_1 = 0.057$	$wR_2 = 0.118$, $R_1 = 0.054$	$wR_2 = 0.116$, $R_1 = 0.047$
R indices (all data)*	$wR_2 = 0.179$, $R_1 = 0.090$	$wR_2 = 0.147$, $R_1 = 0.122$	$wR_2 = 0.133$, $R_1 = 0.099$	$wR_2 = 0.129$, $R_1 = 0.067$
max. diff peak, hole (e/Å^3)	3.067, −0.698	0.800, −0.624	0.727, −0.521	0.391, −0.356

[a] $R_1 = \sum||F_o| - |F_c||/\sum|F_o|$, $wR_2 = \{\sum[w(F_o^2 - F_c^2)^2]/\sum[w(F_o^2)^2]\}^{1/2}$ (sometimes denoted as R_w^2). [b] GooF = $S = \{\sum[w(F_o^2 - F_c^2)^2]/(n - p)\}^{1/2}$, where n is the number of reflections, and p is the total number of refined parameters.

17 was 0.37 g (16%) as a white solid with mp 104.8 °C (dec). ^{1}H NMR (500 MHz, THF-D$_8$, TMS): δ 1.15 (d, $^3J_{P,H} = 13.7$ Hz, 18 H, Me), 1.30 (d, $^3J_{P,H} = 13.8$ Hz, 18 H, Me), 1.68 (m, 12 H, Adamantyl), 1.91 (m, 12 H, Adamantyl), 2.10 (m, 6 H, Adamantyl), 2.20 (m, 4 H, P−CH$_2$). ^{19}F NMR (500 MHz, THF-D$_8$): δ −79.80 (m, 3F), −80.60 (m, 3F). ^{31}P NMR (500 MHz, THF-D$_8$): δ 39.02 (s, 2P). Anal. Calcd for $C_{44}H_{70}F_{12}Ge_2N_2O_3P_2$ (mol wt 1110.25): C, 47.60; H, 6.35; N, 2.52. Found: 47.64; H, 6.41; N, 2.58. The structure was proven by X-ray analysis. The residue from the recrystallizations was subjected to chromatography on silica gel with the eluent petroleum ether/ethyl ether, 10:0.5. 2-[(*P*,*P*-Di-*tert*-butyl-*N*-adamantylphosphinimyl)methyl]-1,1,1,3,3,3-hexafluoropropan-2-ol, **18**. Yield of compound **18** was 1.03 g (26%) as a white solid with mp 82.43 °C (dec). ^{1}H NMR (500 MHz, C$_6$D$_6$, TMS): δ 0.85 (d, $^3J_{P,H} = 12.8$ Hz, 9 H, Me), 0.94 (d, $^3J_{P,H} = 12.9$ Hz, 9 H, Me), 1.50 (m, 6 H, Adamantyl), 1.70 (m, 6 H, Adamantyl), 1.90 (m, 3 H, Adamantyl), 2.20 (m, 2 H, P−CH$_2$). ^{19}F NMR (500 MHz, C$_6$D$_6$): δ −78.07 (m, 3F), −78.41 (m, 3F). ^{31}P NMR (500 MHz, C$_6$D$_6$): δ 84.33 (s, 1P). Anal. Calcd for $C_{22}H_{36}F_6NOP$ (mol wt 475.49): C, 55.57; H, 7.63; N, 2.95. Found: C, 55.74; H, 7.69; N, 3.12. The structure was proven by X-ray analysis.

The Standard Polymerization Procedure. All test samples were prepared under a nitrogen atmosphere. The stock solutions were prepared so that the test concentrations were at a maximum of 10% of the concentration of the stock solution, i.e., 8% stock solution for the precatalyst to test at 7700 ppm. Samples were prepared by taking a known mass of the precatalyst and diluting it with butyl acetate until it reached a total mass for that of the desired percent. The starting materials for the gel time were measured out with 1.95 g of Desmodur (**20**) and 4.74 g of polyol **19**. To this mixture was added the calculated amount of stock solution to produce the desired concentration of the precatalyst, and the contents were mixed. From this, two samples are produced: one is left stirring under a nitrogen atmosphere and the other is left stirring exposed to air. The samples are checked frequently, and the time it took for the samples to gel is recorded for both.

X-ray Diffraction Studies. Data for all structures were collected using a Bruker CCD system at −100 °C. Structure solution and refinement were performed using the Shelxtl[29] set of programs. The Platon-Squeeze[30] program was used to correct the data where the solvent molecules could not be correctly modeled. The residual electron densities for compounds **6** and **14**, which are isostructural, are caused by very weak whole molecule disorder. It is not caused by a poor absorption correction or atoms that have been missed. Because the disorder is weak (∼4−5%), finding other peaks from lighter atoms is impossible and the disordered peaks have not been left in the final refinement. The location of the residual peaks are ∼1.3 Å from a fluorine atom and are not from CF$_3$ disorder. Each asymmetric unit contains two molecules and two disorder peaks. The Sn−Sn or Ge−Ge distances and the distances between disordered peaks are close at 7.84 and 8.17 Å and indicate that in a minor fraction the whole molecules are translated. The structural parameters are reported in Tables 3 and 4.

Acknowledgment. The authors wish to thank Dr. Jerald Feldman for proofreading the manuscript and Vicki North for the DSC measurements.

Supporting Information Available: Crystallographic information (CIF file) for complexes **6**, **9**, **11**, **12**, **14**, **16**, **17**, and **18**. These materials are available free of charge via the Internet at http://pubs.acs.org.

OM060355C

---

(29) Sheldrick, G. *Shelxtl Software Suite*, Version 5.1; Bruker AXS Corp: Madison, WI, 1996.

(30) Spek, A. L. *PLATON*, A Multipurpose Crystallographic Tool; Utrecht University: Utrecht, The Netherlands, 2005.